

Journal Pre-proofs

Manufacture of Tablets with Structurally-Controlled Drug Release using Rapid Tooling Injection Moulding

Erin Walsh, Natalie Maclean, Alice Turner, Moulham Alsuleman, Elke Prasad, Gavin Halbert, Joop H. ter Horst, Daniel Markl

PII: S0378-5173(22)00511-7
DOI: <https://doi.org/10.1016/j.ijpharm.2022.121956>
Reference: IJP 121956

To appear in: *International Journal of Pharmaceutics*

Received Date: 29 January 2022

Accepted Date: 21 June 2022

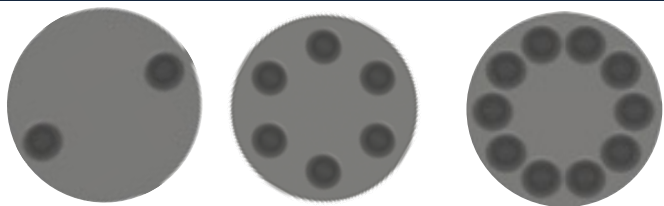
Please cite this article as: E. Walsh, N. Maclean, A. Turner, M. Alsuleman, E. Prasad, G. Halbert, J.H. ter Horst, D. Markl, Manufacture of Tablets with Structurally-Controlled Drug Release using Rapid Tooling Injection Moulding, *International Journal of Pharmaceutics* (2022), doi: <https://doi.org/10.1016/j.ijpharm.2022.121956>

This is a PDF file of an article that has undergone enhancements after acceptance, such as the addition of a cover page and metadata, and formatting for readability, but it is not yet the definitive version of record. This version will undergo additional copyediting, typesetting and review before it is published in its final form, but we are providing this version to give early visibility of the article. Please note that, during the production process, errors may be discovered which could affect the content, and all legal disclaimers that apply to the journal pertain.

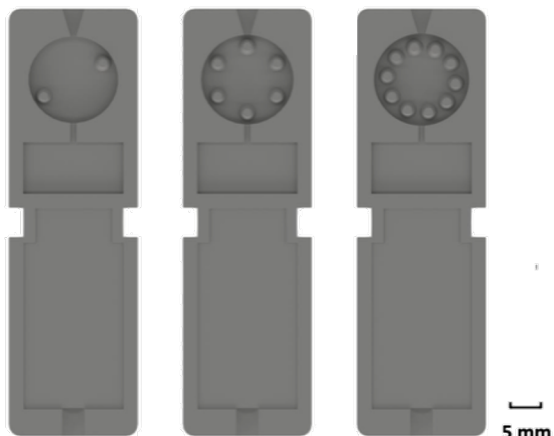
© 2022 Published by Elsevier B.V.



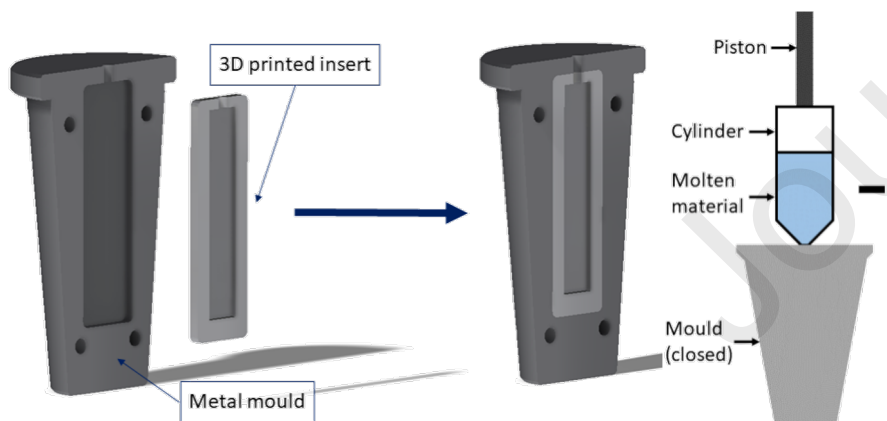
1 Digital Design of Tablets



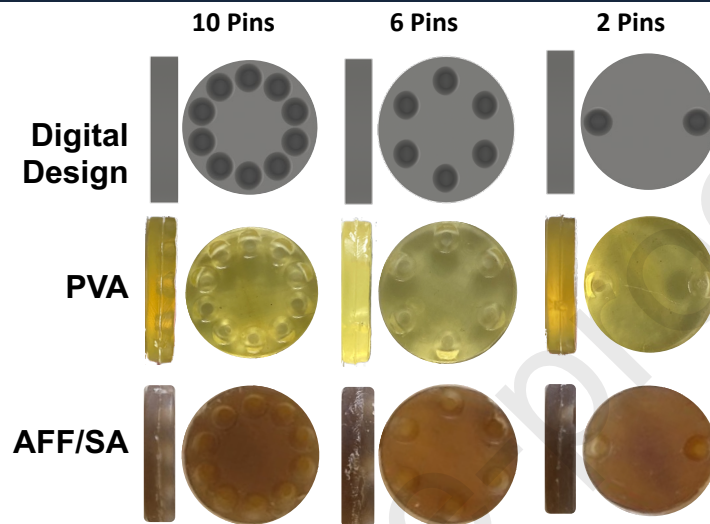
2 Design & 3D Printing of Moulds



3 Integration of 3D Printed Moulds

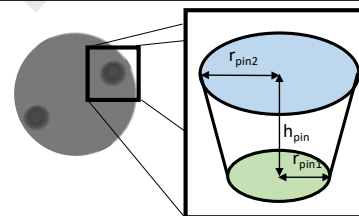


4 Rapid Tooling Injection Moulding

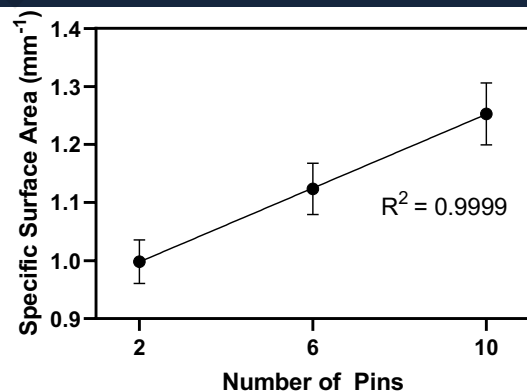


5 Testing: Weight & size

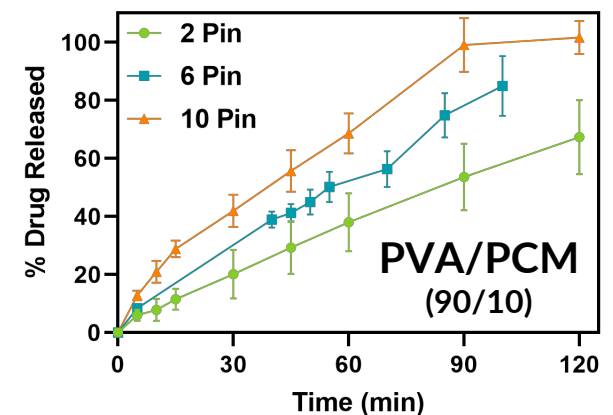
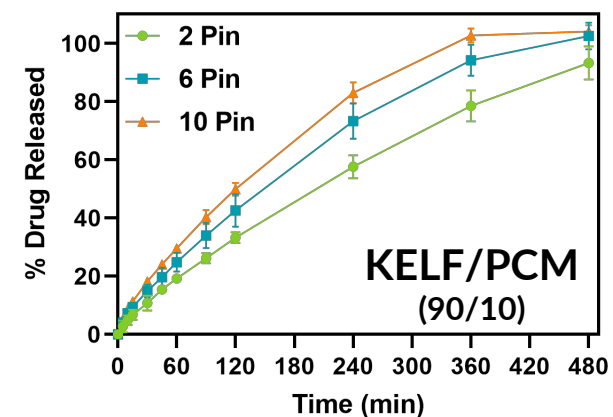
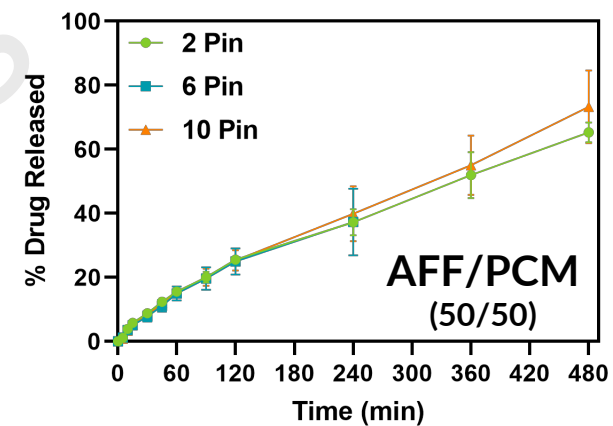
Dimensions
(including OCT)



6 Controlling Specific Surface Area



7 Structurally-Controlled Drug Release



1 Manufacture of Tablets with Structurally-Controlled Drug 2 Release using Rapid Tooling Injection Moulding

3 Erin Walsh^{a,b}, Natalie Maclean^{a,b}, Alice Turner^{a,b}, Moulham Alsuleman^{a,b},
4 Elke Prasad^{a,b}, Gavin Halbert^{a,b}, Joop H. ter Horst^{a,b,c}, Daniel Markl^{a,b,*}

5 ^a*Strathclyde Institute of Pharmacy and Biomedical Sciences, University of Strathclyde, Glasgow, UK*

6 ^b*Future Continuous Manufacturing and Advanced Crystallisation Research Hub, University of
7 Strathclyde, Glasgow, UK*

8 ^c*Laboratoire Sciences et Méthodes Séparatives, Université de Rouen Normandie, Mont Saint Aignan
9 Cedex, France*

10 Abstract

11 With advancements in the pharmaceutical industry pushing more towards tailored
12 medicines, novel approaches to tablet manufacture are in high demand. One of the
13 main drivers towards micro-scale batch production is the ability to fine-tune drug re-
14 lease. This study demonstrates the use of rapid tooling injection moulding (RTIM) for
15 tablet manufacture. Tablets were manufactured with varying structural features to al-
16 ter the surface area whilst maintaining the same volume, resulting in differing specific
17 surface area (SSA). The precision of this technique is evaluated based on eleven poly-
18 mer formulations, with the tablets displaying <2% variability in mass. Further tablets
19 were produced containing paracetamol in three different polymer-based formulations to
20 investigate the impact of SSA on the drug release. Significant differences were observed
21 between the formulations based on the polymers polyvinyl alcohol (PVA) and Klucel
22 ELF. The polymer base of the formulation was found to be critical to the sensitivity
23 of the drug release profile to SSA modification. The drug release profile within each
24 formulation was modified by the addition of structural features to increase the SSA.

25 *Key words:* injection moulding, rapid tooling, specific surface area, additive
26 manufacture, dissolution

*Corresponding Author: daniel.markl@strath.ac.uk

27 1. Introduction

28 The interest in manufacturing micro-scale batches of pharmaceutical products contin-
29 ues to heighten with the growth of the personalised medicine and clinical trials market.
30 The development and manufacture of products for small patient populations using tra-
31 ditional large scale industrial production processes is currently not cost effective and
32 hence hinders the progress in this area. Novel technologies to manufacture micro-scale
33 batches in a sustainable manner are needed. One such technique is additive manufactur-
34 ing (AM), commonly referred to as 3D printing. This technique is able to produce tablets
35 with complex geometries allowing formulators to adjust the dose and modify the drug
36 release profiles by varying the specific surface area of the dosage form (Goyanes et al.,
37 2015; Karasulu and Ertan, 2002). Another manufacturing technology with potential to
38 produce micro-scale batches is injection moulding (IM) coupled with hot melt extrusion
39 (HME). IM is a widely applied manufacturing technique in the plastics industry and has
40 been utilised in the pharmaceutical industry to produce solid oral dosage forms (Bartlett
41 et al., 2017; Quinten et al., 2009; Zema et al., 2012). The manufacturing benefits of us-
42 ing IM to make pharmaceutical drug products include reduced microbial contamination
43 alongside greater freedom in defining the size and shape of the dosage form (Zema et al.,
44 2012). In addition, IM allows the production of solid dispersions and solutions which can
45 increase the rate of release of the drug and hence improve bioavailability (Quinten et al.,
46 2009). This aspect is critically important for current and future medicines as approx-
47 imately 70% of new drug candidates in the development pipeline show poor solubility
48 (Loftsson and Brewster, 2010).

49 The IM process uses heat to encourage a thermoplastic material to adopt the desired
50 geometry. Thermoplastics are a particularly large collection of materials with unique
51 thermal, mechanical and electrical characteristics (Giboz et al., 2007; Hecke and Schom-
52 burg, 2004). The differing material properties of these thermoplastic materials therefore
53 need to be understood to utilise them effectively in an IM-based process. Pressure-
54 volume-temperature behaviour, polymer structure, morphology and crystallinity are all
55 material properties that will have a major impact on the IM process (Annicchiarico and
56 Alcock, 2014). A number of process parameters involved in IM impact the viscosity of
57 the thermoplastic material such as shear stress, shear rate, temperature and pressure.

58 Besides the solubility of the drug substance, the drug release of oral solid dosage
59 forms made through IM are influenced by the formulation and the specific surface area
60 (SSA) (Goyanes et al., 2015; Martinez et al., 2018; Quinten et al., 2009). The SSA can be
61 modified by adjusting the surface area of the tablet while keeping the volume constant.
62 Alterations to the SSA can be achieved by designing structural features into the surface
63 of the tablet, which can be realised using micro-IM. Micro-IM is used when an object
64 contains either a mass of a few milligrams, μm -scale features or objects where dimensional
65 tolerances are in the μm range (Giboz et al., 2007; Packianather et al., 2015).

66 The IM process (standard and micro) requires an appropriate mould that defines the
67 shape of the final product. Traditional metal mould-making is a time-consuming process
68 which is both cost and skill exhaustive (Rani et al., 2018). In most cases this limits the
69 optimisation of moulds, which is a crucial step in identifying a suitable product structure
70 with micro-features that meets the performance specifications. Requirements on the
71 fabrication of the mould and its material include the ability to create precise micro-
72 structures and it must be sufficiently hard and ductile to survive the injection moulding
73 process (Heckele and Schomburg, 2004). Developments in additive manufacturing have
74 opened the door for rapid tooling in IM as an alternative to traditional metal moulds
75 (Rani et al., 2018). Rapid tooling is defined as being the use of additive manufacturing
76 techniques for the manufacture of moulds directly (direct tooling) or to create a pattern
77 which is then used to manufacture a mould (indirect tooling) (Rani et al., 2018; Mendible
78 et al., 2017; Qayyum et al., 2017). With additive manufacturing techniques now utilising
79 photopolymers to print objects with high resolution, the potential for this technique to
80 be used to manufacture moulds for micro-IM is apparent (Mohan et al., 2017; Surace
81 et al., 2021). In order for these materials to be suitable for use in micro-IM, there
82 must be sufficient resistance to both the temperature and pressure experienced during
83 the injection process (Bartlett et al., 2017). Photopolymer-based additive manufacture
84 techniques were selected due to the material properties of the photoresins used, i.e.
85 photoresins are expected to have high thermal resistance and superior surface quality
86 making them a good choice for rapid tooling (Bartlett et al., 2017). Previous work
87 by Walsh et al. (2021) demonstrated that stereolithography (SLA) can produce mould
88 inserts suitable for use in conjunction with IM and suggests printing recommendations

89 for this purpose. The integration of rapid tooling and injection moulding (Rapid Tooling
90 Injection Moulding or RTIM) reduces the overall cost and the lead-time that comes with
91 using traditional metal moulds (Mendible et al., 2017; Formlabs, 2016). The coupling of
92 these technologies makes low production runs economically feasible and also allows for a
93 more agile approach to research (Mendible et al., 2017; Formlabs, 2016).

94 The objectives of this work were to develop a process for producing solid oral dosage
95 forms with structural features designed to control SSA using the RTIM technique and
96 assess its suitability to adjusting the drug release behaviour. Three different geometries
97 of dosage forms were produced using ten different pharmaceutical grade polymers which
98 are typically used in HME, IM and additive manufacture. The relationship between
99 drug release and SSA was assessed for three different paracetamol formulations, each
100 containing a different polymer. The processability of these materials was assessed as was
101 the accuracy and precision of the process in reference to the digital design of the tablets.

102 **2. Materials and Methods**

103 *2.1. Materials*

104 *2.1.1. Stereolithography Additive Manufacture*

105 The photoresin used in this work is Clear v4 from Formlabs (Massachusetts, USA)
106 based on the findings from (Walsh et al., 2021). Isopropyl alcohol (Sigma Aldrich, USA)
107 is used to wash the moulds post-printing.

108 *2.1.2. Rapid Tooling Injection Moulding*

109 A number of raw materials were used in this work as detailed in Table 1. The materials
110 used are pharmaceutical-grade except LDPE. LDPE is included as a reference material
111 as it has been widely studied in the literature of IM and micro-IM. The acronym for each
112 material will be used throughout this manuscript to refer to a particular material.

113 The majority of the formulations used in this work required preparation via HME
114 to ensure molecular level mixing prior to feeding the material into the RTIM system. A
115 series of formulations comprised solely of polymers or polymers with plasticising agents
116 were produced and are detailed in Table 2. The API-containing formulations used in this
117 work are detailed in Table 3.

Table 1: List of raw materials, their supplier details and their acronyms as used in this study.

Material	Supplier	Acronym
Affinisol HPMC HME 15LV	The Dow Chemical Company, USA	AFF
Eudragit E PO	Evonik, Germany	EPO
Klucel EF	Ashland, USA	KEF
Klucel ELF	Ashland, USA	KELF
Klucel LF	Ashland, USA	KLF
Low-density Polyethylene	Sigma Aldrich, USA	LDPE
Polyethylene	Sigma Aldrich, USA	PE
Polyethylene Glycol 4000	Sigma Aldrich, USA	PEG
Polyvinyl alcohol	Sigma Aldrich, USA	PVA
Soluplus [®]	BASF, Germany	SOL
Sorbitol Emprove Parteck SI 150	Merck, USA	SOR
Stearic Acid	Sigma Aldrich, USA	SA
Paracetamol	Mallinckrodt, UK	PCM

118 2.2. Methods

119 2.2.1. Stereolithography Additive Manufacture

120 Mould inserts were printed, as previously reported, using the Form 2 (Formlabs,
 121 Massachusetts) stereolithography (SLA) printer (Walsh et al., 2021). The moulds are
 122 printed at a 45° angle from the build platform. On completion of printing, the moulds
 123 were washed in isopropyl alcohol in an agitated wash bath for a period of 10 minutes
 124 before being left to dry completely. The moulds were then removed from the build
 125 platform and placed in the FormCure (Formlabs) for 60 minutes at 60°C. Supporting
 126 material was removed and any surface roughness on the rear of the mould surface was
 127 lightly sanded.

128 2.2.2. Design of Tablet Geometries

129 Three different mould insert designs were produced for this study (see Figure 1) to
 130 modify the tablet geometry. Conical frustum shaped ‘pins’ (Figure 2c) were added to the

Table 2: List of polymer-based formulations, their preparation method and their acronyms that will be used in this manuscript. Composition ratios are given in brackets by weight.

Primary Polymer	Plasticiser	Prep Method	Acronym
Affinisol	-	HME	AFF
Affinisol (85%)	Polyethylene Glycol (15%)	HME	AFF/PEG 85/15
Affinisol (85%)	Stearic acid (15%)	HME	AFF/SA 85/15
Affinisol (85%)	Polyethylene (15%)	HME	AFF/PE 85/15
Eudragit EPO (85%)	Polyethylene Glycol (15%)	HME	EPO/PEG 85/15
Klucel EF	-	HME	KEF
Klucel ELF	-	HME	KELF
Klucel LF	-	HME	KLF
Polyvinyl Alcohol	-	HME	PVA
Soluplus (85%)	Sorbitol (15%)	HME	SOL/SOR 85/15

Table 3: List of paracetamol formulations and their acronyms that will be used in this manuscript. Composition ratios are given in brackets by weight.

Formulation	Acronym
Affinisol (50%) + Paracetamol (50%)	AFF/PCM 50/50
Klucel ELF (90%) + Paracetamol (10%)	KELF/PCM 90/10
Polyvinyl Alcohol (90%) + Paracetamol (10%)	PVA/PCM 90/10

131 designs in increasing number ($n = 2, 6$ or 10 for the three tablet geometries). In order
 132 to maintain the tablet mass across all three designs for a formulation, the volume of the
 133 three designs was kept constant. The diameter of the tablet was adjusted to account for
 134 the reduction in volume resulting from the introduction of the pins. The thickness of
 135 each tablet was kept constant for all three designs as were the dimensions of each pin.

136 The basic design of the tablet geometries comprised a cylindrical tablet with the
 137 conical frustum pins cut into the top surface (Figure 2).

138 The surface area of the tablets was calculated using the following equation:

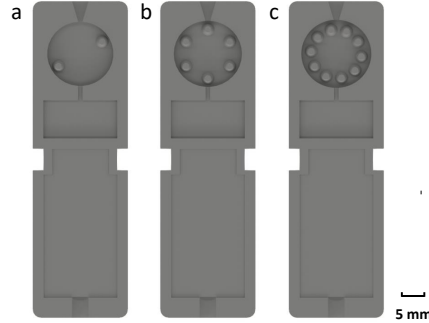


Figure 1: The three mould designs used in this study. a) 2 Pin b) 6 Pin c) 10 Pin.

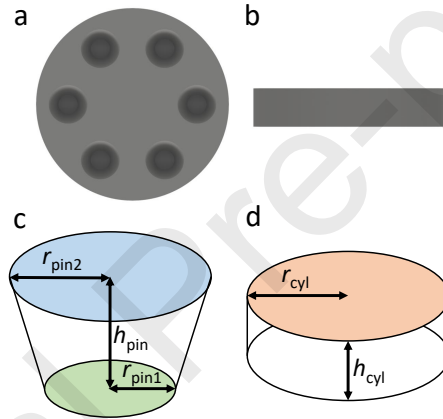


Figure 2: Schematic of tablet design features. a) A top and b) side view of a tablet produced from the 6 Pin design; c) design of an individual pin; d) design of the basic cylindrical tablet structure.

$$A_{\text{tab}} = 2\pi r_{\text{cyl}} h_{\text{cyl}} + 2\pi r_{\text{cyl}}^2 + n\pi \left[r_{\text{pin1}}^2 - r_{\text{pin2}}^2 + (r_{\text{pin1}} + r_{\text{pin2}}) \sqrt{(r_{\text{pin1}} - r_{\text{pin2}})^2 + h_{\text{pin}}^2} \right], \quad (1)$$

139 where A_{tab} is the tablet surface area, r_{cyl} is the radius of the cylinder, h_{cyl} is the
 140 height of this cylinder, n is the number of pins, r_{pin1} is the top radius of the pin, r_{pin2} is
 141 the bottom radius of the pin and h_{pin} is the depth of the pin.

142 The volume of the tablets was calculated using the following equation:

$$V_{\text{tab}} = 2\pi r_{\text{cyl}}^2 h_{\text{cyl}} - \left(\frac{1}{3} \pi n h_{\text{pin}} (r_{\text{pin1}}^2 + r_{\text{pin2}}^2 + r_{\text{pin1}} r_{\text{pin2}}) \right), \quad (2)$$

143 where V_{tab} is the tablet volume, r_{cyl} is the radius of the cylinder, h_{cyl} is the thickness
 144 of the cylinder, n is the number of pins, h_{pin} is the depth of the pin, r_{pin1} is the top
 145 radius of the pin and r_{pin2} is the bottom radius of the pin.

146 The specific surface area was calculated as the ratio between the surface area to the
 147 volume:

$$SSA_{\text{tab}} = \frac{A_{\text{tab}}}{V_{\text{tab}}} \quad (3)$$

148 Full details of the tablet dimensions produced from these designs can be found in
 149 Table 4.

Table 4: Summary table of tablet dimensions.

Design Feature	2 Pin Design	6 Pin Design	10 Pin Design
Diameter (mm)	15.23	15.69	16.12
Thickness (mm)	3	3	3
Volume (mm ³)	530.03	529.82	529.80
Surface Area (mm ²)	527.48	592.76	658.08
Number of Pins	2	6	10
Pin Depth (mm)	2	2	2
Pin Radius 1 (mm)	1.5	1.5	1.5
Pin Radius 2 (mm)	0.75	0.75	0.75
Specific Surface Area (mm ⁻¹)	1.00	1.12	1.24

150 2.2.3. Rapid Tooling Injection Moulding

151 The RTIM process couples SLA with IM. Mould inserts, produced via SLA, are housed
 152 within a metal mould casing (Figure 3). Also visible are a number of design features on
 153 the printed mould insert to make it suitable for use in the RTIM process. The tablet
 154 cavity is the section of the mould insert which will produce the tablet. The air cavity
 155 provides an overflow space for any excess injection material and offers a space for the air

156 to compress upon moulding. The removal points can be found on each side of the mould,
 157 these aid in removing the mould inserts from the metal moulds. The separation point at
 158 the bottom of the mould inserts is used to separate the two halves of the mould insert.

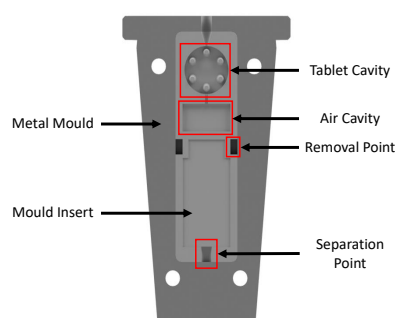


Figure 3: The mould insert for the 6 Pin Design inserted into the metal mould. This depiction represents one half of the full mould.

159 The two halves of the metal mould were pieced together and placed into the HAAKE
 160 MiniJet Pro Piston Injection Moulding System (Thermo Fisher Scientific, USA) which
 161 is an upright air-pressurised injection moulder. The injection material is placed into the
 162 melt cylinder, the piston is attached and this is then placed into the injection moulder.
 163 A number of processing parameters must be set:

- 164 • Cylinder temperature to which the injection material will be heated to.
- 165 • Mould temperature to which the mould will be heated to.
- 166 • Injection pressure which will be applied to the piston to move the injection material
 167 into the mould.
- 168 • Injection time is the length of time for which the injection pressure will be applied.
- 169 • Hold pressure which will be applied after the injection material has filled the mould.
- 170 • Hold time is the length of time for which the hold pressure will be applied.

171 These processing parameters vary for different injection materials (see Table 5). For
 172 all formulations the injection time, hold pressure and hold time were kept constant at
 173 10 s, 50 bar and 10 s, respectively.

Table 5: RTIM process parameters used for each of the formulations. Formulations marked with * required the addition of an aerosol silicone-based lubricant to aid removal from the mould. The API-containing formulations are given below the double horizontal line.

Formulation	Cylinder Temp	Mould Temp	Injection Pressure
AFF*	N/A	N/A	N/A
AFF/PEG 85/15*	200 °C	100 °C	150 bar
AFF/SA 85/15*	180 °C	100 °C	150 bar
AFF/PE 85/15*	180 °C	100 °C	150 bar
EPO/PEG 85/15*	N/A	N/A	N/A
KEF	140 °C	70 °C	150 bar
KELF	140 °C	70 °C	150 bar
KLF	140 °C	70 °C	150 bar
PVA*	200 °C	70 °C	200 bar
SOL/SOR 85/15*	N/A	N/A	N/A
AFF/PCM 50/50*	130 °C	70 °C	150 bar
KELF/PCM 90/10*	120 °C	70 °C	150 bar
PVA/PCM 90/10*	180 °C	100 °C	200 bar

174

175 A number of formulations (see formulations marked with * in Table 5) required the
 176 application of a silicone based lubricant onto the surface of the mould inserts to aid
 177 removal of the injected material. Upon completion of injection, the metal mould is
 178 removed from the injection moulder, the metal mould opened and the mould insert
 179 removed. When sufficiently cooled, the mould insert is opened and the tablet removed
 180 from the mould cavity.

181 2.2.4. Gravimetric Analysis

182 All tablets were weighed on a four decimal point balance (Entris II, Sartorius). The
 183 masses reported reflect the average of each batch produced. The mean and standard

184 deviations reported are $n = 18$ for all formulations.

185 *2.2.5. Dimensional Analysis*

186 The diameter and thickness of each tablet was measured using a digital calliper (Sci-
187 enceware Digi-Max, Sigma Aldrich). A total of three diameter and three thickness mea-
188 surements were taken for each tablet, the measurements shown are an average of these
189 replicates. The mean and standard deviations reported were $n = 18$ for all other formu-
190 lations.

191 *2.2.6. Optical Coherence Tomography*

192 A spectral-domain optical coherence tomography (OCT) system (GAN600 Series,
193 Thorlabs, New Jersey, USA) equipped with a LK3-BB (focal length: 36 mm) was used
194 to measure the actual pin dimensions. OCT produces cross-sectional images of a sample
195 which can be used for depth measurements. The lateral resolution is $\approx 4 \mu\text{m}$, the axial
196 resolution in air is $\approx 3 \mu\text{m}$ and the image size is a 1024 x 1024 pixels with a x -axis pixel
197 size of $5.86 \mu\text{m}$ and a y -axis pixel size of $1.95 \mu\text{m}$. The OCT probe was focused over
198 the pins on the tablet surface and a 2D cross-section image was acquired. The focus
199 is adjusted to ensure a strong signal. The diameters (see Figure 2c) at both the top
200 and bottom surfaces and the depth of the pins were measured. The mean and standard
201 deviations are reported for 18 samples for all formulations.

202 *2.2.7. Dissolution*

203 Dissolution testing was performed using an ADT8i Dissolution bath (USP II) paddle
204 on a closed loop setting with a T70+ UV/Visible spectrophotometer (Automated Lab
205 Systems, UK). Each vessel contained 1000 mL of 50 mM KH_2PO_4 adjusted to pH 5.8
206 with NaOH. Dissolution testing was performed at 37°C with a paddle speed of 50 rpm.
207 Samples were automatically drawn at a rate of 20 mL/min through the sampling pump
208 with a flush volume of 20 mL and with cannula filters of $20 \mu\text{m}$ (ALS, UHMW PE, Part
209 No 50831). Samples were measured at timepoints of 5 min, 10 min, 15 min, 30 min,
210 1 hr, 2 hr, 4 hr, 6 hr and 8 hr. UV detection of PCM was performed at a wavelength of
211 243 nm through a 1 mm flow cell cuvette. For each formulation, 6 tablets were tested.
212 Standards of 0.2 mg/mL PCM in phosphate buffer were prepared in duplicate.

213 All tablets were weighed and their weights recorded. A standard verification of both
214 PCM standards produced was performed prior to the dissolution assay, with the ab-
215 sorbance values for both standards recorded.

216 3. Results

217 3.1. Gravimetric Analysis

218 The mass across the three designs was designed to be constant for a given formulation
219 as the volume was constant across the three tablet geometries. Variations of the calcu-
220 lated volume across the three designs were $<2.5\%$ across all formulations (Table S1-6 in
221 the supplementary information). No data is shown for the AFF, EPO/PEG 85/15 and
222 SOL/SOR 85/15 formulations as they were unprocessable via this RTIM process (more
223 details are provided in the Discussion section). The average mass varied between formula-
224 tions due to different true densities of the materials used. The variation in mass observed
225 across all formulations and all designs was well within the pharmacopoeia standards (\pm
226 5% of the tablet core weight) for tablet mass variation (Figure 4a)(The International
227 Pharmacopoeia, 2019). Figure 4b demonstrates the tablet to tablet variability within
228 the LDPE tablets. A total of 60 tablets are displayed, showing that even within this
229 larger batch size, the mass variation is low ($\pm 0.58\%$) and the RTIM process produces
230 consistent and uniform tablets.

231 Generally, a higher degree of variation was observed for the Affinisol-based formula-
232 tions (Figure 4c). This was attributed to the difficulty in processing these tablets. These
233 formulations had a tendency to stick to the mould surface if not removed while warm
234 leading to a reduced uniformity of mass compared to the other formulations tested. While
235 the AFF/PEG formulation had the highest standard deviation across all formulations
236 ($\pm 1.87\%$), the masses still fell within the pharmacopoeia limits (Figure 4b).

237 3.2. Dimensional Analysis

238 All formulations demonstrated high accuracy and precision to the digital designed
239 thickness value of 3 mm, i.e. $<99.84\%$ of designed value with a standard deviation of
240 $\pm 0.88\%$ across all formulations and geometries. The Affinisol-based formulations pro-
241 duced values slightly higher than the design value (100.70% of design) and the mea-
242 surements had a slightly higher standard deviation ($\pm 0.81\%$) than for non-AFF based

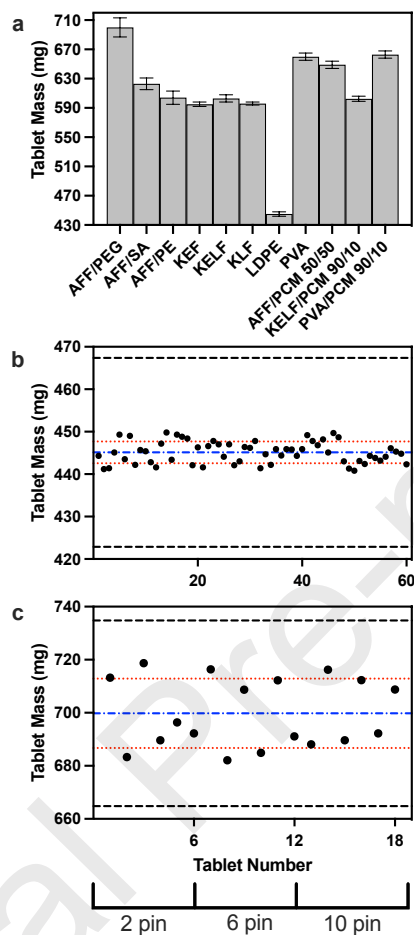


Figure 4: Tablet mass of RTIM tablets. a) The average mass of all tablets for each formulation. Error bars represent the standard deviation ($n = 60$ for LDPE, $n = 18$ for all other formulations). b) The mass of 60 LDPE tablets. c) the mass of 18 AFF/PEG tablets. The blue dotted lines represent the average tablet weight of this batch with the upper and lower red dotted lines being the average plus or minus the standard deviation respectively. The black dotted lines represents the upper and lower pharmacopoeia limit (in this case taken as tablet weight $\pm 5\%$).

243 formulations ($\pm 0.30\%$) which is attributed to the difficulty associated with processing
 244 these formulations as previously discussed. As above, no data is shown for the AFF,
 245 EPO/PEG 85/15 and SOL/SOR 85/15 formulations.

246 All formulations demonstrated good accuracy and precision to the digital designed
 247 diameter values across all three tablet geometries (range from $98.68 \pm 0.42\%$ to 99.71

248 $\pm 0.23\%$ of the intended values).

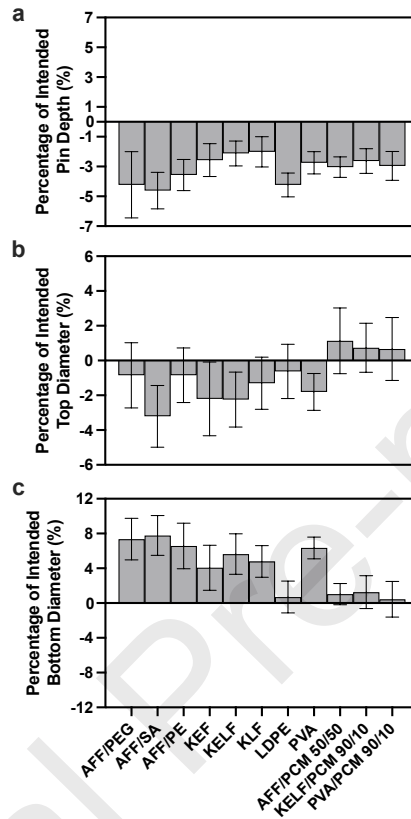


Figure 5: Tablet pin characteristics measured by OCT. a) The depth of the pins on the tablet surface (h_{pin} from Figure 2c) b) The top surface diameter of the pins on the tablet surface ($2 \times r_{\text{pin1}}$ from Figure 2c) c) The bottom surface diameter of the pins on the tablet surface ($2 \times r_{\text{pin2}}$ from Figure 2c). a-c: for each bar $n = 6$ measurements with the error bars representing the standard deviation.

249 The depth, top diameter and bottom diameter of the pins in all three geometries
 250 were measured using OCT. Both the depth of the pins and the bottom diameter (as seen
 251 in Figure 5a and c respectively) were below the expected values across all formulations.
 252 The top diameter of the pins (as seen in Figure 5b) was generally above the expected
 253 value of 3 mm across all formulations. While the measured values deviated slightly from
 254 the designed values, the low values of the standard deviations across all measurements
 255 suggest that the variability within the batches was small.

256 Figure 6 displays the three tablet geometries for PVA and AFF/SA formulations. It
 257 is worth noting that for the AFF based formulations, the RTIM process is not considered
 258 optimised and the colouration on the tablets produced is indicative of thermal degrada-
 259 tion of the AFF polymer. Reduction of the processing temperatures would reduce this
 260 polymeric degradation and result in dosage forms having a lighter colour.

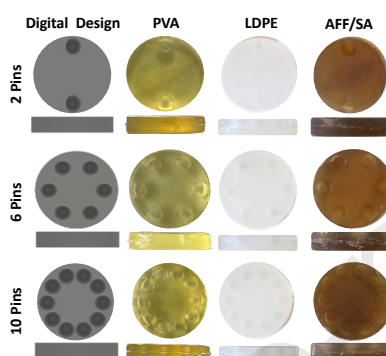


Figure 6: Physical tablets produced for three of the formulations trialled.

261 From the dimensional analysis, the surface area, volume and specific surface area
 262 (Figure 7) were calculated using Equations 1, 2 and 3. Full details of the equations used
 263 to calculate these parameters and the propagation of errors can be found in section S2
 264 of the supplementary information.

265 3.3. Dissolution

266 Dissolution studies were conducted for each tablet geometry on the three PCM for-
 267 mulations (Figure 8). From this study, no significant differences in the drug release
 268 profiles of AFF/PCM 50/50 could be detected from the three tablet geometries trialled.
 269 On the contrary, significant differences in the rate of drug release were observed between
 270 the different tablet geometries for KELF/PCM 90/10 (Figure 8b) and PVA/PCM 90/10
 271 (Figure 8c) formulations.

272 Due to the asymmetric nature of the dosage forms produced in this work, there are
 273 two distinct faces. The release profile can be influenced by the orientation of the tablet
 274 in the dissolution vessel. Only dissolution data of tablets with the face up (pins on top)
 275 were used in the results shown here. The first face is that which has the pins indented

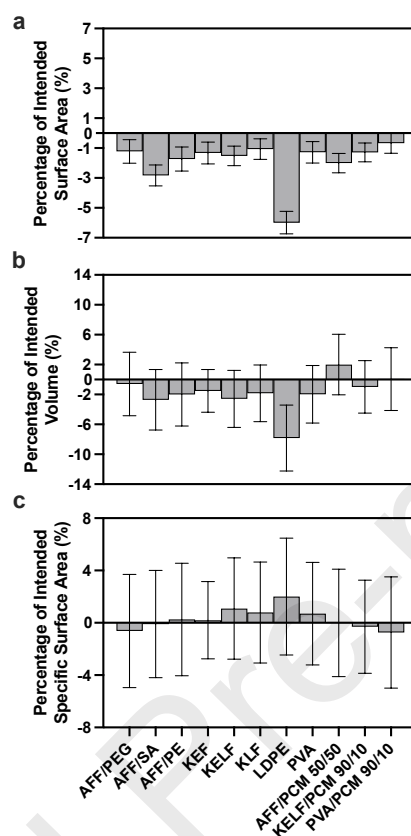


Figure 7: Analysis of the actual surface area, volume and specific surface area compared to the digital design. a) The average surface area for each formulation as calculated by Equation 1. b) The average volume for each formulation as calculated by Equation 2. c) The average specific surface area for each formulation as calculated by Equation 3. a-c: for each bar, $n = 18$ tablet with the error bars representing the propagated standard deviation.

276 into the surface, and the second face is the flat cylindrical base. This asymmetry of the
 277 tablets presented some challenges during the dissolution studies. All of the tablets were
 278 positioned with the pin-face upwards when the dissolution studies were conducted. The
 279 system which was used for this work operates to drop the tablets into the dissolution
 280 vessels simultaneously. When the tablets fall, some come to rest in the base of the vessels
 281 with the pin-face upwards, and others with the pin-face downwards (see Figure 9a). The
 282 tablets which were pin-face downwards demonstrated slower drug release (see Figure 9b),
 283 which is attributed to the reduced access of the dissolution media to the surface micro-

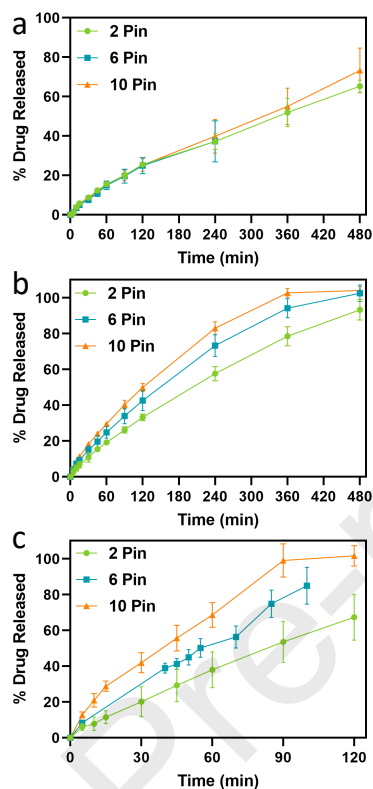


Figure 8: Drug release profiles for a) AFF/PCM 50/50, b) KELF/PCM 90/10 formulation and c) PVA/PCM 90/10 formulation. All: Symbols represent the mean of $n = 6$ tablets (with the exception of PVA/PCM 90/10, for which $n = 4$ as discussed in Section S3 of the supplementary information) with the error bars showing 95% confidence intervals. In b), data collection of AFF/PCM 50/50 formulations was terminated after the 240 min time point for the 6 Pin geometry due to errors with the dissolution apparatus. In c), the sample time points for the 6 Pin geometry differ to those of the 2 Pin and 10 Pin geometries due to running errors with the dissolution apparatus.

284 features and differing hydrodynamics on the two faces of the tablet.

285 For future studies, the tablets could manually be placed into the dissolution vessels
 286 to avoid these inconsistencies. Putting micro-features on both faces of the tablet surface
 287 would likely reduce the errors associated with the asymmetry. However, the blocked face
 288 would still have limited liquid access and therefore the full impact of the increase in SSA
 289 would not be clear from such a set up. It is however worth stating that this issue is not
 290 an issue that would be encountered in vivo.

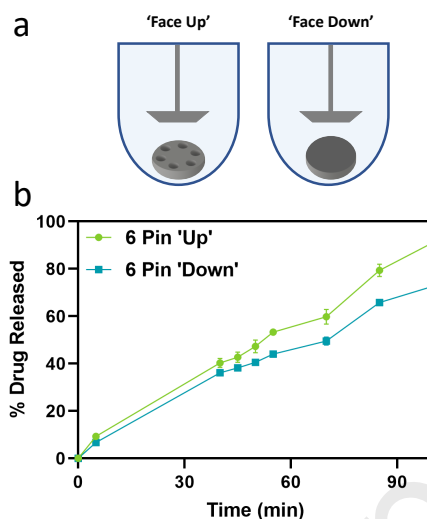


Figure 9: Impact of anisotropic tablet structure on drug release profiles of the PVA/PCM 90/10 formulation. a) A depiction of the 'Face Up' and 'Face Down' orientation that tablets may adopt in the dissolution vessels b) 6 Pin PVA/PCM 90/10 tablets split by 'Face up' and 'Face down'. Sample size for 'Face up' is 4 tablets and for 'Face down' is 2 tablets. Error bars represent the 95% confidence intervals.

291 4. Discussion

292 4.1. Formulation Processability in RTIM

293 Three of the formulations trialled were deemed to be unprocessable: AFF, EPO/PEG
 294 85/15 and SOL/SOR 85/15. For the AFF formulation, the main challenge was associated
 295 with the temperatures and pressures required to process the material. The temperatures
 296 and pressures required to achieve a workable viscosity of the formulation were too high
 297 for the mould materials to withstand, causing fracture of the plastic mould inserts and
 298 ultimately resulting in an unsuccessful RTIM process. EPO/PEG 85/15 and SOL/SOR
 299 85/15, adhered strongly to the surface of the printed mould. While this is an issue
 300 that was encountered with a number of other formulations (those marked with * in
 301 Table 5), the addition of the silicon-based lubricant was not able to overcome the issues.
 302 For the EPO/PEG 85/15 and SOL/SOR 85/15 formulations a number of processing
 303 parameters were trialled including varying the temperatures for both the cylinder and the
 304 mould, reducing the injection pressure and the injection time. No successful processing
 305 conditions could be found for these materials in this specific RTIM process. The extent

306 of the adhesion to the printed mould surface was such that the two mould halves were
307 fused together. As such, removal of the tablets from these moulds was not possible and
308 the formulations were deemed unprocessable. Further studies could investigate whether
309 inclusion of a gap in the mould design would prevent the mould from fusing and facilitate
310 the separation of the mould and removal of the tablet for formulations which are prone
311 to high levels of adhesion.

312 *4.2. Physical Parameters of the Tablets*

313 Theoretically, all formulations should produce physical parameters which match the
314 digital design. The digitally designed volume was constant across the three geometries,
315 while the surface area and specific surface area increased with the increased number of
316 pins.

317 There are a number of factors which create uncertainty in these calculated values.
318 Primarily, there is an inherent uncertainty that arises from the printing of the plastic
319 mould inserts which was extensively studied in (Walsh et al., 2021). Additionally, there
320 are measurement errors associated with the different techniques used to measure the di-
321 mensions of the tablets. The uncertainty arising from the measurements alone attributes
322 22.79% of the uncertainty on volume, 24.11% for surface area and 22.82% for specific sur-
323 face area. Finally, there are errors associated with the different formulations used. This
324 is most apparent when looking at the mass variability of the formulations, where some
325 have significantly higher standard deviations than others. The only variable changed in
326 that case is the formulation so it can be assumed that the difference in standard devia-
327 tion is attributed solely to the formulation differences. These formulation differences are
328 likely driven by density differences between the formulations, caused by different polymer
329 structures, rheology and packing, as well as the interactions between the polymers and
330 plasticisers. It may be possible that these effects could be mitigated by incorporating a
331 correction factor to adjust the mould design for a given formulation.

332 Figure 7a and b depicts the calculated values for surface area, volume and specific
333 surface area for all formulations. The specific surface area demonstrated high accuracy
334 and precision across all formulations trialled. With the exception of LDPE, both the
335 surface area and volume data demonstrate a high degree of both accuracy and precision
336 to the digital design. The LDPE formulation was found to have a lower surface area and

337 volume than the digital design. The accuracy of the LDPE formulation was therefore
338 lower than the others tested however the precision of the measurements remained high.
339 As polyethylene (and therefore LDPE) is a semi-crystalline thermoplastic, this can be
340 attributed to shrinkage on cooling which is characteristic of crystalline polymers (De
341 Santis et al., 2010). While the shrinkage resulting in a reduced diameter was clear, there
342 was some evidence of the thickness value also being lower than anticipated and lower than
343 all other formulations tested. This shrinkage is expected to be highest on the longest axis
344 which for these designs would be the diameter. The specific surface area demonstrated
345 high accuracy and precision across all formulations trialled. Even in the case of LDPE,
346 where reduced accuracy was observed for surface area and volume, the deficit to both
347 was such that the specific surface area fell much closer to the digitally designed value.

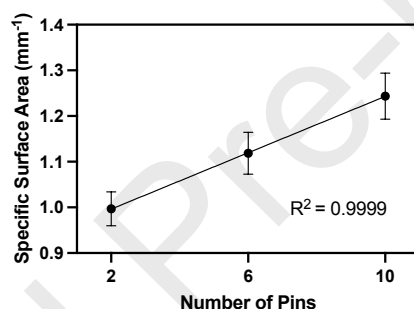


Figure 10: The average specific surface area for all formulations vs. the number of pins in the tablet geometry. Error bars represent the standard deviation.

348 The relationship between the number of pins featured in the design and the resultant
349 specific surface area is highly linear producing an R^2 of 0.99 based on the data collected for
350 all formulations trialled in this study (Figure 10). This indicates that further modification
351 of the specific surface area could be achieved via this pin-based approach with a high
352 degree of accuracy.

353 4.3. Drug Release Analysis

354 The AFF/PCM 50/50 formulation generally had a slow drug release, failing to reach
355 100% release after the 8 hour time period the dissolution test was conducted for. Based
356 on the data collected, the AFF/PCM 50/50 results do not show a clear difference in

357 drug release rate for tablets with 2, 6 or 10 pins. A similar study by Prasad et al.
358 (2019) assessed the dissolution performance of 3D printed AFF tablets containing 10%
359 and 50% wt. PCM. In this study, different tablet geometries (cylindrical, rectangular
360 grids with and without slotted shapes) with different SSAs were manufactured. It was
361 demonstrated that drug release was fastest with increasing SSA for these designs (Prasad
362 et al., 2019), whereas the AFF/PCM tablets tested in this study do not follow the same
363 trend. This may be attributed to the large dose of PCM (~320 mg for AFF/PCM,
364 compared to ~60 mg for PCM/KELF and PCM/PVA formulations, and 17 and 80 mg
365 in the AFF-based formulations tested by Prasad et al. (2019)). It should also be noted
366 that the release behaviour can be influenced by the manufacturing method and hence
367 differences in the drug release profiles between the 3D printed tablets and the RTIM
368 tablets may not exclusively be caused by the different drug loadings.

369 Significant differences were observed across the drug release profiles of both KELF/PCM
370 90/10 and PVA/PCM 90/10 formulations with different numbers of pins. This finding
371 is in agreement with other studies, in which increasing SSA was found to increase the
372 rate of drug release (Goyanes et al., 2015; Reynolds et al., 2002). The time to reach 50%
373 drug release for each formulation is shown in Figure 11. For formulations containing
374 PVA and KELF, increasing the SSA resulted in a decrease in the time to release 50% of
375 the drug. As discussed above, this trend is not displayed for the AFF-based formulation.
376 This suggests that the polymer used in the formulation has a significant impact on both
377 the sensitivity to changes in SSA and the absolute time for drug release. This could be
378 attributed to the higher dose of PCM in the AFF formulation compared to KELF or
379 PVA-based tablets. The mechanism of drug release influences the sensitivity to changes
380 in SSA (e.g. diffusion, erosion, and swelling), however further studies would be required
381 to investigate the release mechanisms as these can be influenced by the API, formulation,
382 tablet size and geometry, and the manufacturing process.

383 *4.4. Capabilities and Limitations of RTIM for Solid Oral Dosage Form Fabrication*

384 RTIM produces tablets with very low interparticle (uncontrolled) porosity within
385 the dosage form that enables a tight control of the available surface area and hence
386 release behaviour. Even minor changes in the surface area can thus influence the release
387 behaviour as shown in this study.

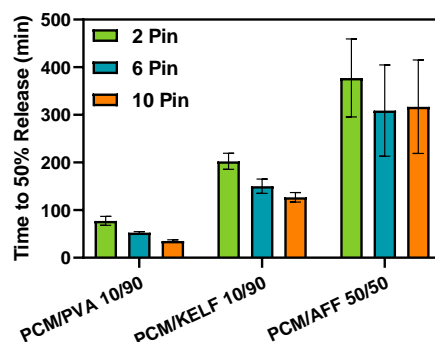


Figure 11: The time taken for formulations to reach 50% drug release for each formulation split by tablet geometry.

388 Additionally, RTIM presents the potential for an increased formulation space, com-
 389 pared to other techniques that allow the customisation of the structure such as FDM.
 390 Typically, the drug loading that can be achieved for FDM printing is low due to the
 391 necessity for the print filament to possess the correct properties for successful printing
 392 (Zhang et al., 2018, 2017; Korte and Quodbach, 2018; Aho et al., 2019). There have
 393 however been cases where a higher drug loading has been achieved (Prasad et al., 2019).
 394 Additionally, in most cases these filament properties also limit which polymers can be
 395 used in conjunction with FDM, further reducing the formulation space available for FDM
 396 (Zhang et al., 2018). Further work on material development will be required to expand
 397 the formulation space of FDM (Gioumouxouzis et al., 2019). For example, a recent paper
 398 by Zheng et al. (2021) demonstrated a novel 3D printing process that aims to mitigate
 399 some of the challenges of traditional FDM approaches and allows for the manufacture of
 400 tablets from excipient and API powders, without the need for filaments. RTIM on the
 401 other hand is not dependent on the filament properties and thus higher drug loadings and
 402 a wider range of polymer carriers can be used without further research and development.
 403 This will greatly expand the formulation space and allow a greater variety of drugs, drug
 404 loadings and polymers to be utilised for more complex dosage form geometries.

405 It must be mentioned that the RTIM process is not without its limitations. The major
 406 limitation of this technique is the current throughput. Both the RTIM and FDM pro-
 407 cesses require material preparation via hot melt extrusion, however RTIM also requires

408 the printing of the mould inserts which adds significant time. The actual production of
409 the tablets however is typically faster for RTIM, with a single tablet able to be produced
410 every 1-2 minutes while for FDM this is in the 4-5 minute range (Zhang et al., 2017;
411 Korte and Quodbach, 2018). Both of these times quoted would be for a formulation
412 considered to be favourable, an unfavourable formulation would extend these production
413 times further. The throughput of RTIM could be improved by utilising it as a develop-
414 ment tool for a more traditional μ IM process using a tooled steel mould. This would
415 allow for a far more efficient process and enable the direct coupling with HME. While the
416 structural flexibility for RTIM is considered high due to the ability to create accuracy
417 and precise surface micro-features, it must also be noted that internal features would be
418 far more difficult to produce. Therefore, there are structural and geometric limitations
419 with the RTIM technique. Despite not having the constraints of the filament properties
420 that FDM has, RTIM has additional limitations such as the material rheology and the
421 tendency for some materials to stick to the mould inserts. Even with these drawbacks,
422 the RTIM process displays clear potential to produce dosage forms with highly accurate
423 and precise physical structures.

424 5. Conclusion

425 The RTIM method produced tablets from a variety of thermoplastic pharmaceutical
426 grade polymers. These tablets were close to the digital designs in terms of their dimen-
427 sions, surface area, volume and specific surface area. The mass variability of all tablets
428 produced was low and well within the limits of the pharmacopoeia. The specific surface
429 areas of the tablets produced were accurate to the digital designs suggesting that this
430 RTIM process can be used to produce tablets of designed geometries for the purpose of
431 fine-tuning drug release profiles. RTIM has proven to be an accurate and precise method
432 for the production of tablets with a desired specific surface area.

433 The RTIM method was capable of producing drug-loaded tablets from pharmaceutical
434 polymer-based formulations. It is well known that for many formulations, drug release
435 kinetics are dependent on the specific surface area of the tablets (Goyanes et al., 2015;
436 Martinez et al., 2018; Prasad et al., 2019; Pires et al., 2020). As such, to refine the
437 drug release behaviour, the control of the specific surface area must be accurate. This

438 has been achieved through addition and modification of pins into the tablet geometry
439 and subsequent altering of the overall tablet diameter. The decision as to whether the
440 RTIM process is the most appropriate is application dependent. Consideration of the
441 accuracy, precision, material requirements and throughput amongst other factors should
442 be carefully examined when deciding the most appropriate manufacture technique for
443 the desired application. These factors will directly influence the throughput, cost and
444 overall quality and trueness to the digital design. Evidence suggests that RTIM can be
445 used successfully for low production runs of <500 parts, and for larger batches it can
446 be used as a development tool to obtain the desired tablet design prior to producing a
447 traditional tooled steel mould for scaled up production (Rahmati and Dickens, 2007).

448 **Acknowledgements**

449 For the purpose of open access, the author has applied a Creative Commons At-
450 tribution (CC BY) licence to any Author Accepted Manuscript version arising from
451 this submission. The authors would like to thank EPSRC and the Future Continuous
452 Manufacturing and Advanced Crystallisation Research Hub (Grant Ref EP/P006965/1),
453 EPSRC DTP (Grant Ref EP/N509760/1), EPSRC Strategic Equipment (Grant Ref
454 EP/S02168X/1), Royal Society (Grant Ref RSG/R2/180276) and the University of Strath-
455 clyde for funding this research. The authors would like to acknowledge that this work was
456 carried out in the CMAC National Facility supported by UKRPIF (UK Research Part-
457 nership Fund) award from the Higher Education Funding Council for England (HEFCE)
458 (Grant Ref HH13054).

459 **Declaration of Competing Interest**

460 The authors declare that they have no known competing financial interests or personal
461 relationships that could have appeared to influence the work reported in this paper.

462 **References**463 **References**

- 464 A. Goyanes, R. Martínez-Pacheco, P. Robles, A. Buanz, A. W. Basit, S. Gaisford, Effect of geometry
 465 on drug release from 3D printed tablets, *International Journal of Pharmaceutics* 494 (2015) 657–663.
 466 doi:10.1016/j.ijpharm.2015.04.069.
- 467 H. Y. Karasulu, G. Ertan, Different geometric shaped hydrogel theophylline tablets: Statistical approach
 468 for estimating drug release, *Farmaco* 57 (2002) 939–945. doi:10.1016/S0014-827X(02)01297-1.
- 469 L. Bartlett, E. Grunden, R. Mulyana, J. Castro, A Preliminary Study On The Performance Of Additive
 470 Manufacturing Tooling For Injection Moulding, in: *SPE ANTEC*, 2017, pp. 100–104.
- 471 T. Quinten, T. D. Beer, C. Vervaet, J. P. Remon, Evaluation of injection moulding as a pharmaceutical
 472 technology to produce matrix tablets, *European Journal of Pharmaceutics and Biopharmaceutics* 71
 473 (2009) 145–154. doi:10.1016/j.ejpb.2008.02.025.
- 474 L. Zema, G. Loreti, A. Melocchi, A. Maroni, A. Gazzaniga, Injection Molding and its application to drug
 475 delivery, *Journal of Controlled Release* 159 (2012) 324–331. doi:10.1016/j.jconrel.2012.01.001.
- 476 T. Loftsson, M. E. Brewster, Pharmaceutical applications of cyclodextrins: basic science and product de-
 477 velopment, *Journal of Pharmacy and Pharmacology* 62 (2010) 1607–1621. doi:10.1111/j.2042-7158.
 478 2010.01030.x.
- 479 J. Giboz, T. Copponnex, P. Mélé, Microinjection molding of thermoplastic polymers: A review, *Journal*
 480 *of Micromechanics and Microengineering* 17 (2007) 96–109. doi:10.1088/0960-1317/17/6/R02.
- 481 M. Hecke, W. K. Schomburg, Review on micro molding of thermoplastic polymers, *Journal of Mi-*
 482 *cromechanics and Microengineering* 14 (2004). doi:10.1088/0960-1317/14/3/R01.
- 483 D. Annicchiarico, J. R. Alcock, Review of factors that affect shrinkage of molded part in injection
 484 molding, *Materials and Manufacturing Processes* 29 (2014) 662–682. doi:10.1080/10426914.2014.
 485 880467.
- 486 P. R. Martinez, A. Goyanes, A. W. Basit, S. Gaisford, Influence of Geometry on the Drug Release
 487 Profiles of Stereolithographic (SLA) 3D-Printed Tablets, *AAPS PharmSciTech* 19 (2018). doi:10.
 488 1208/s12249-018-1075-3.
- 489 T. Quinten, T. D. Beer, J. P. Remon, C. Vervaet, Overview of Injection Molding As a Manufacturing
 490 Technique for Pharmaceutical Applications, *Innovation* (2009) 1–42.
- 491 M. Packianather, C. Griffiths, W. Kadir, Micro injection moulding process parameter tuning, in:
 492 *Procedia CIRP*, 2015. doi:10.1016/j.procir.2015.06.093.
- 493 A. Rani, A. Majdi, K. Altaf, F. Ahmad, J. Ahmad, Enhanced Polymer Rapid Tooling for Metal Injection
 494 Moulding Process, in: *3rd International Conference on Progress in Additive Manufacturing*, 2018,
 495 pp. 656–661. doi:10.25341/D4J014.
- 496 G. A. Mendible, J. A. Rulander, S. P. Johnston, G. A. Mendible, J. A. Rulander, S. P. Johnston,
 497 Comparative study of rapid and conventional tooling for plastics injection molding, *Rapid Prototyping*
 498 *Journal* 23 (2017) 344–352. doi:10.1108/RPJ-01-2016-0013.
- 499 J. A. Qayyum, K. Altaf, A. M. Abdul Rani, F. Ahmad, M. Jahanzaib, Performance of 3D printed

- 500 polymer mold for metal injection molding process, *ARNP Journal of Engineering and Applied Sciences*
501 12 (2017) 6430–6434. doi:10.3390/met8060433.
- 502 M. Mohan, M. N. Ansari, R. A. Shanks, Review on the Effects of Process Parameters on Strength,
503 Shrinkage, and Warpage of Injection Molding Plastic Component, *Polymer - Plastics Technology and*
504 *Engineering* 56 (2017). doi:10.1080/03602559.2015.1132466.
- 505 R. Surace, V. Basile, V. Bellantone, F. Modica, I. Fassi, Micro injection molding of thin cavities using
506 stereolithography for mold fabrication, *Polymers* 13 (2021). URL: [https://www.mdpi.com/2073-4360/](https://www.mdpi.com/2073-4360/13/11/1848)
507 [13/11/1848](https://www.mdpi.com/2073-4360/13/11/1848). doi:10.3390/polym13111848.
- 508 E. Walsh, J. H. ter Horst, D. Markl, Development of 3D Printed Rapid Tooling for Micro-Injection
509 Moulding, *Chemical Engineering Science* (2021) 116498. doi:10.1016/j.ces.2021.116498.
- 510 Formlabs, Moldmaking with 3D Prints - Techniques for Prototyping and Production, Technical Report,
511 Formlabs, 2016.
- 512 The International Pharmacopoeia, 5.2 Uniformity of mass for single-dose preparations, World Health
513 Organisation (2019) 1–2. URL: <https://apps.who.int/phint/2019/index.html#p/home>.
- 514 F. De Santis, R. Pantani, V. Speranza, G. Titomanlio, Analysis of shrinkage development of a semicrys-
515 talline polymer during injection molding, *Industrial and Engineering Chemistry Research* 49 (2010)
516 2469–2476. doi:10.1021/ie901316p.
- 517 E. Prasad, M. T. Islam, D. J. Goodwin, A. J. Megarry, G. W. Halbert, A. J. Florence, J. Robertson,
518 Development of a hot-melt extrusion (HME) process to produce drug loaded Affinisol™ 15LV filaments
519 for fused filament fabrication (FFF) 3D printing, *Additive Manufacturing* 29 (2019). doi:10.1016/j.
520 *addma*.2019.06.027.
- 521 A. Goyanes, J. Wang, A. Buanz, R. Martínez-Pacheco, R. Telford, S. Gaisford, A. W. Basit, 3D Printing
522 of Medicines: Engineering Novel Oral Devices with Unique Design and Drug Release Characteristics,
523 *Molecular Pharmaceutics* (2015). doi:10.1021/acs.molpharmaceut.5b00510.
- 524 T. D. Reynolds, S. A. Mitchell, K. M. Balwinski, Investigation of the effect of tablet surface area/volume
525 on drug release from hydroxypropylmethylcellulose controlled-release matrix tablets, *Drug Develop-*
526 *ment and Industrial Pharmacy* 28 (2002) 457–466. doi:10.1081/DDC-120003007.
- 527 J. Zhang, A. Q. Vo, X. Feng, S. Bandari, M. A. Repka, Pharmaceutical Additive Manufacturing: a
528 Novel Tool for Complex and Personalized Drug Delivery Systems, *AAPS PharmSciTech* 19 (2018)
529 3388–3402. doi:10.1208/s12249-018-1097-x.
- 530 J. Zhang, X. Feng, H. Patil, R. V. Tiwari, M. A. Repka, Coupling 3D printing with hot-melt extrusion
531 to produce controlled-release tablets, *International Journal of Pharmaceutics* 519 (2017) 186–197.
532 doi:10.1016/j.ijpharm.2016.12.049.
- 533 C. Korte, J. Quodbach, Formulation development and process analysis of drug-loaded filaments man-
534 ufactured via hot-melt extrusion for 3D-printing of medicines, *Pharmaceutical Development and*
535 *Technology* 23 (2018) 1117–1127. doi:10.1080/10837450.2018.1433208.
- 536 J. Aho, J. P. Bøtker, N. Genina, M. Edinger, L. Arnfast, J. Rantanen, Roadmap to 3D-Printed Oral Phar-
537 maceutical Dosage Forms: Feedstock Filament Properties and Characterization for Fused Deposition
538 Modeling, *Journal of Pharmaceutical Sciences* 108 (2019) 26–35. doi:10.1016/j.xphs.2018.11.012.

- 539 C. I. Gioumouxouzis, C. Karavasili, D. G. Fatouros, Recent advances in pharmaceutical dosage forms
540 and devices using additive manufacturing technologies, *Drug Discovery Today* 24 (2019) 636–643.
541 doi:10.1016/j.drudis.2018.11.019.
- 542 Y. Zheng, F. Deng, B. Wang, Y. Wu, Q. Luo, X. Zuo, X. Liu, L. Cao, M. Li, H. Lu, S. Cheng,
543 X. Li, Melt extrusion deposition (med™) 3d printing technology – a paradigm shift in design and
544 development of modified release drug products, *International Journal of Pharmaceutics* 602 (2021)
545 120639. doi:10.1016/j.ijpharm.2021.120639.
- 546 F. Q. Pires, I. Alves-Silva, L. A. Pinho, J. A. Chaker, L. L. Sa-Barreto, G. M. Gelfuso, T. Gratieri,
547 M. Cunha-Filho, Predictive models of FDM 3D printing using experimental design based on phar-
548 maceutical requirements for tablet production, *International Journal of Pharmaceutics* 588 (2020)
549 119728. doi:10.1016/j.ijpharm.2020.119728.
- 550 S. Rahmati, P. Dickens, Rapid tooling analysis of Stereolithography injection mould tooling, *Internation-
551 al Journal of Machine Tools and Manufacture* 47 (2007) 740–747. doi:10.1016/j.ijmachtools.
552 2006.09.022.

CRedit Author Statement

Erin Walsh: Conceptualization, Investigation, Formal Analysis, Methodology, Visualization, Writing - Original Draft; **Natalie Maclean:** Writing - Review & Editing, Visualization; **Alice Turner:** Methodology, Writing - Review & Editing; **Moulham Alsuleman:** Methodology, Writing - Review & Editing; **Elke Prasad:** Methodology, Writing - Review & Editing; **Gavin Halbert:** Supervision, Writing - Review & Editing; **Joop H. ter Horst:** Supervision, Conceptualization, Writing - Review & Editing; **Daniel Markl:** Supervision, Conceptualization, Writing - Review & Editing, Project administration, Funding acquisition

Declaration of interests

The authors declare that they have no known competing financial interests or personal relationships that could have appeared to influence the work reported in this paper.

The authors declare the following financial interests/personal relationships which may be considered as potential competing interests:

Erin Walsh reports financial support was provided by Engineering and Physical Sciences Research Council. Daniel Markl reports a relationship with The Royal Society that includes: funding grants.